JOURNAL OF APPLIED ELECTROCHEMISTRY 22 (1992) 21–27

Electrochemical oxidation of manganese(II) at a platinum electrode

W.-H. KAO*, V. J. WEIBEL

RAYOVAC Corporation, Madison, WI53711, USA

Received 20 November 1990; revised 20 April 1991

Electrochemical oxidation of Mn^{2+} in sulphuric acid to form MnO_2 was studied using stationary and rotating platinum/platinum ring-disc electrodes. It appears that nucleation of MnO_2 is governed by an equilibrium involving a Mn(III) intermediate. Growth of MnO_2 involves the reduction of MnO_2 surfaces by Mn^{2+} ions in the solution to form MnOOH intermediates. The subsequent electrochemical oxidation of MnOOH releases a hydrogen ion and results in the formation of MnO_2. The rate constant of MnOOH oxidation to MnO_2 was estimated to be $40\,s^{-1}$. With a sufficient supply of Mn^{2+} ions, a layer of MnOOH is built up and the in-solid diffusion of hydrogen ions becomes the rate-determining-step. With a low Mn^{2+} concentration, diffusion of Mn^{2+} ions from bulk electrolyte to the MnO_2/electrolyte interface is a factor controlling the growth of MnO_2. The activation energy and the pre-exponential term of the diffusion coefficient of Mn^{2+} in 0.5 M sulphuric acid were determined to be $44.8\,kJ\,mol^{-1}$ and $100\,cm^2\,s^{-1}$, respectively.

1. Introduction

Electrolytic manganese dioxide (EMD) is a very important cathode material for high performance dry cells. Typically, it is deposited on an inert anode from an acidic bath containing manganese sulphate at a temperature around 90° C [1]. A number of mechanistic studies of this reaction have been published in the literature [2–12], some of which provide contradictory interpretations of the results. EMD is nonstoichiometric and possibly contains bound water [13] and low valent manganese oxides [14, 15] such as MnOOH. In industrial practice, dispersed fine MnO_2 particles can be seen in the bath and in the lines of spent electrolyte. These dispersed particles are not believed to originate from the electrode surface. They are more likely the product of a secondary chemical reaction involving intermediates in the electrolyte.

The conception of the electrochemical oxidation of Mn^{2+} in dilute sulphuric acid to form EMD has changed from a mediated oxidation to a direct oxidation. The mediators proposed in the fifties, such as hydroxyl radicals [2] and persulphate ions [3], were questioned by later investigators simply because the thermodynamic potentials for the formation of the mediators were higher than that of Mn^{2+} oxidation to MnO_2 [16]. Zaretskii *et al.* [4] proposed a direct oxidation of Mn^{2+} to Mn^{3+} or Mn^{4+}. Mn^{3+} underwent disproportionation to produce Mn^{2+} and Mn^{4+} which was hydrolyzed to form MnO_2. Thermodynamically, Mn^{2+} oxidation forming MnO_2 can proceed at a lower potential than that to either Mn^{3+} or Mn^{4+}. Fleischmann *et al.* [5] explained this difference in potential by assuming that Mn^{3+} and Mn^{4+} intermediates were adsorbed on the electrode surface. The subsequent dehydration of the adsorbed Mn^{4+} ions forming MnO_2 was the rate-determining step (r.d.s.). Growth of MnO_2 proceeded three-dimensionally. A mechanism involving multi-step dissociation of adsorbed manganese(IV) hydroxides was offered.

Sugimori *et al.* [6] suggested that MnOOH was an intermediate in Mn^{2+} oxidation to MnO_2. Sato *et al.* [7] proposed that Mn^{2+} reduced the MnO_2 surface to form MnOOH which was then oxidized electrochemically to MnO_2. Jorgensen [8] argued that the r.d.s. of EMD deposition was electron conduction through the semiconducting MnO_2 deposit. Paul and Cartwright [9, 10] speculated the formation of porous solid intermediates like MnOOH, Mn_2O_3 and $Mn(OH)_4$ during oxidation of Mn^{2+} on growing MnO_2. Mn^{2+} diffused through the porous layer to the MnO_2 surface for oxidation. A steady state was established when the diffusion rate of Mn^{2+} into the pores matched the conversion rate of the intermediates to MnO_2. They estimated the thickness of the intermediate layer, based on the results of impedance measurements and rotating-ring-disc experiments [10], to be 2 to 10 μm. At this laboratory, solid MnO_2 less than 10 μm thick had been successfully deposited onto a smooth titanium electrode substrate. X-ray diffraction analysis of the deposit, accumulated from several runs, revealed only the presence of γ-MnO_2.

Grzegorzewski and Heusler [11] investigated MnO_2 electrodes using a rotating quartz frequency balance and concluded that charge transfer of manganous and oxygen ions were statistically independent steps and water was built into the oxides. The temperature and acidic strength applied in their study were far lower than those practiced in production [1]. Using

* To whom correspondence should be addressed at: Johnson Controls, Inc., Milwaukee, WI 53201, USA.

0021-891X/92 $03.00 + .12

surface-enhanced Raman spectroscopy, Gosztola and Weaver [12] identified intermediates of MnOOH and Mn(IV)–O–Mn(III) species during reduction of several equivalent monolayers of MnO_2 to $Mn(OH)_2$. They claimed that $Mn(OH)_2$ could be reoxidized to form MnO_2 via the MnOOH intermediate.

Experiments were conducted in this lab to study the electrochemical oxidation of Mn^{2+} at a platinum electrode. Carbon or titanium anodes are normally used to produce EMD. Carbon is subject to corrosion at a high anodic potential in sulphuric acid and can be damaged during removal of the MnO_2 deposit. The history and surface cleanliness of a titanium electrode are critical to production of EMD. Etching and cleaning of a titanium electrode after each harvest cycle are necessary to obtain consistent results. Because of the above drawbacks in these materials, a platinum electrode was chosen for this study. After all, when the electrode was completely covered with EMD, deposition essentially occurred on a MnO_2 electrode. The electrode substrate simply acted as a current collector and had no contribution to the growth of MnO_2. Cyclic voltammetry and chronoamperometry of Mn^{2+} oxidation in sulphuric acid at stationary and rotating-ring-disc platinum electrodes at temperatures ranging from 80 to 95° C are reported.

2. Experimental details

A platinum/platinum rotating-ring-disc electrode (RRDE) (Pine Instrument Company, Grove City, PA) with a geometric disc area of 0.46 cm^2 was used. The ring-disc electrode (RDE) was first polished with a 1 μm diamond compound (Buehler Ltd, Lake Bluff, IL) and then rinsed thoroughly with deionized water (DI water). The electrode was next treated in 1 M sulphuric acid by cycling repetitively between -0.2 and $+1.4$ V against an Ag/AgCl (saturated KCl) reference electrode at a scan rate of 500 mV s^{-1} until a static current-potential profile previously described [17] was obtained. The electrode was then oxidized at about $+1.5$ V with respect to Ag/AgCl for 2 min and stored in 1 M sulphuric acid. Prior to the experiments, the electrode was reduced at -0.2 V against Ag/AgCl in 1 M H_2SO_4 for 2 min to remove the oxide layer before transferring to the test solutions. This reduced electrode is herein defined as the clean platinum electrode. The measured collection efficiency of this RDE, using the ferri-ferrocyanide redox system, was 0.153.

A Pine RDE4 dual potentiostat (Pine Instrument Company, Grove City, PA) and a PARC 173 potentiostat with a PARC 175 Universal Programmer (Princeton Applied Research Corp., Princeton, NJ) were used for potential control. The ring potential was held constant at either $+0.6$ V or $+0.7$ V. An Omnigraphic 2000 (Houston Instrument, Irvine, CA) and Gould 3054 X–Y recorder (Gould Inc., Rolling Meadows, IL) were used for data acquisition. The experimental error in current measurements was typically less than 5%. All the electrode potentials in the text are referred to an Ag/AgCl (saturated KCl) reference electrode.

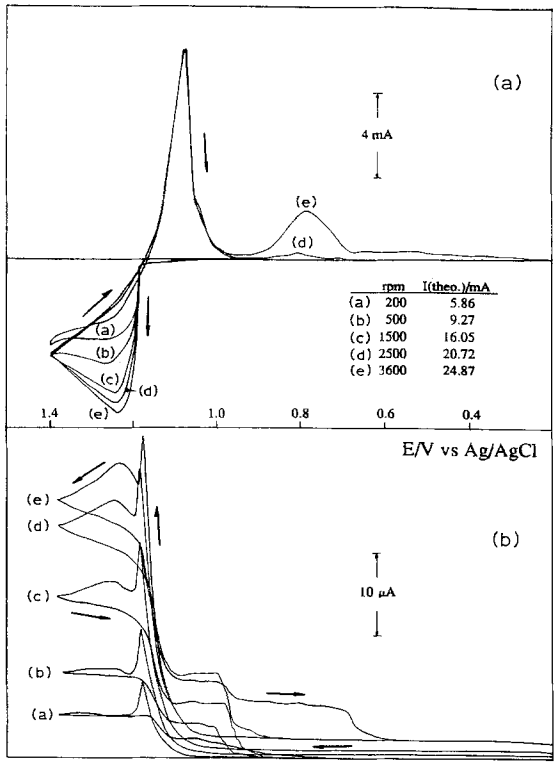

Fig. 1. CV's of Mn^{2+} oxidation and reduction of MnO_2 deposit at the (a) platinum disc, and (b) ring electrodes. The electrolyte contains 10 mM $MnSO_4$ and 0.5 M H_2SO_4 at 90° C. Scan rate is 10 mV s^{-1}. The ring potential is held constant at $+0.6$ V with respect to Ag/AgCl.

Manganous sulphate and sulphuric acid were analytical reagents from Fisher Scientific (Pittsburgh, PA). DI water was used for preparation of solutions. The temperature of the electrolyte, ranging from 80 to 95° C, was sustained using a heating mantle and was controlled within ± 1° C. The rotation rate applied to the electrode was between 0 and 3600 r.p.m.

3. Results

The temperature for EMD deposition is typically between 88° C and the boiling point of the electrolyte. We extended the range to room temperature to obtain more kinetic information. However, MnO_2 deposition became inconsistent at temperatures lower than 80° C. Peeling and loss of MnO_2 deposits were frequently observed. Therefore, the low temperature limit in this study was set at 80° C.

3.1. *Cyclic voltammetry*

Figure 1a shows typical disc cyclic voltammograms (CVs) for Mn^{2+} oxidation and reduction of MnO_2 deposits in sulphuric acid at 90° C at different rotation rates. The profile of CVs at other temperatures was the same. The onset of oxidative current in the anodic scan was about 1.05 V. Around 1.18 V, the current rose sharply until the maximum was reached at a potential beyond 1.22 V. A similar sharp rise in oxidative current was also observed at both a glassy carbon and a smooth titanium electrode [18]. The foot

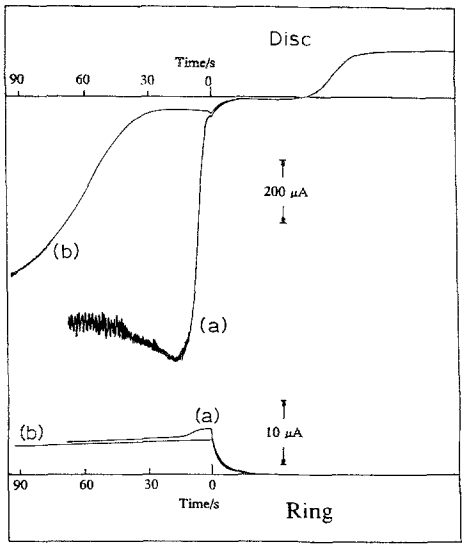

Fig. 2. Current as a function of time for Mn^{2+} oxidation at the platinum/platinum RDE in 0.5 M H_2SO_4 with 10 mM $MnSO_4$ at 80° C. The disc potential is scanned at a rate of 10 mV s^{-1} from 0 V to (a) 1.173 V and (b) 1.164 V and then held constant. Time is set at zero when the scan is terminated. The ring potential is constant at 0.6 V with respect to Ag/AgCl. The rotation rate is 200 r.p.m.

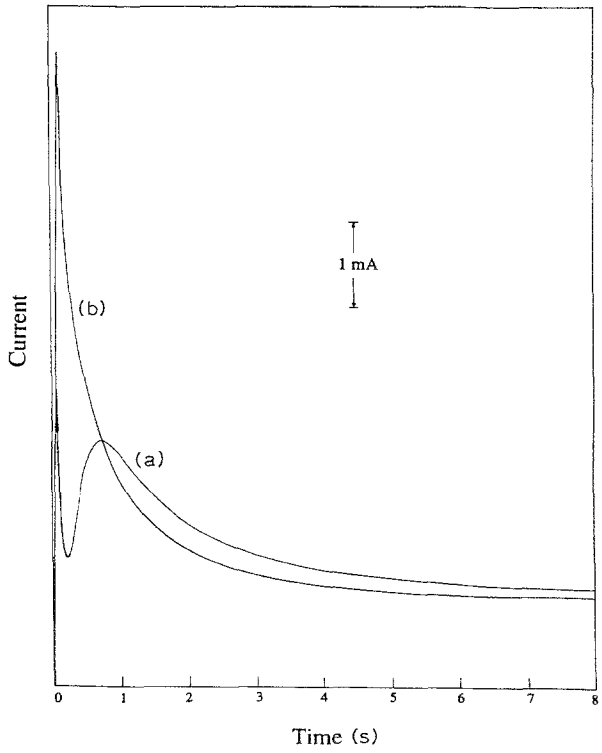

Fig. 3. Current against time for Mn^{2+} oxidation at the (a) clean, and (b) MnO_2 coated platinum electrode in 0.5 M H_2SO_4 with 10 mM $MnSO_4$ at 80° C. Potential of the electrode is stepped from 0.70 to 1.24 V with respect to Ag/AgCl.

potential at which current rises sharply is herein defined as the critical potential. The anodic current stayed relatively constant to the switching potential at low rotation rates but decayed at high rotation rates. Regardless of the rotation rate the current seemed to approach a limiting value at high voltages before the onset of oxygen evolution. The disc current decayed in the reverse scan and crossed over the anodic waves at a potential between 1.2 and 1.1 V before the reduction of MnO_2 deposits.

The peak potential of MnO_2 reduction was about 1.08 V. Additional waves at less positive potentials were observed at high rotation rates. Irrespective of the rotation rate and oxidative charge passed during the anodic sweep, the shape of the first reduction peak was the same. The peak was somewhat symmetrical and the half-wave-width was about 55 mV, equivalent to that of a two-electron ideal Nernstian reduction of strongly adsorbed species [19]. The charge under the first reduction peak, corrected for the background, was 32% to 41% of the oxidative charge in the anodic sweep. This ratio was as high as 55% if the additional reductive wave was included. The charge ratio suggested one-electron reduction of the MnO_2 deposit.

The corresponding ring currents are shown in Fig. 1b. The ring currents initially rose with the disc currents and then dropped abruptly to form "peaks" at the critical potentials. The collection efficiency of the rising ring current was consistent with the theoretical value. Beyond 1.18 V, when EMD deposition occurred, the collection efficiency was in the order of 10^{-3}. In the reverse scan a finite ring current, which increased with rotation rate, was detected.

3.2. *Effects of applied anodic potential*

MnO_2 could be formed at a potential less positive than the critical potential. As shown in Fig. 2, the disc potential scan from 0 V to a potential between 1.05 and 1.18 V was stopped and then held constant. This constant potential is herein defined as the "end potential". The disc current started rising and the deposition of EMD was observed after a period of induction time. The induction time required for deposition to take place was a function of the end potential, being longer for a less positive value. When the end potential approached the critical potential the induction time became very sensitive to the end potential. The ring current, on the other hand, stayed relatively constant after the termination of the potential scan.

3.3. *Chronoamperometry*

An example of the chronoamperometric study on Mn^{2+} oxidation at a stationary electrode is shown in Fig. 3. When a potential step from 0.70 V to various anodic potentials was applied to a clean electrode, an induction period was observed. The induction time was shorter for higher applied overvoltage. MnO_2 continued to grow after the induction period until diffusion of Mn^{2+} from the bulk electrolyte became a limiting factor. When the same potential step was applied to an electrode pre-coated with a layer of MnO_2, no induction time was observed and the current decay followed the Cottrell equation (Curve b, Fig. 3). The diffusion coefficients of Mn^{2+} in 0.5 M H_2SO_4 at 80, 90 and 95° C were measured from the current decay to be 2.38×10^{-5}, 3.55×10^{-5}, and 4.47×10^{-5} cm^2 s^{-1}, respectively. The diffusional activation energy and the pre-exponential term were then determined from the Arrhenius plot to be 44.8 kJ mol^{-1} and 100 cm^2 s^{-1}, respectively.

3.4. *Effects of rotation rates, soak time, and scan rate*

The Levich plot of the data from Fig. 1 is shown in Fig. 4. In one experiment a constant anodic charge sufficient to generate a 0.15 μm thick MnO_2 deposit was passed in 20 s. The electrode was removed, rinsed with DI water, soaked in sulphuric acid containing various concentrations of Mn^{2+} for a period of time and rinsed again. The electrode was then transferred to sulphuric acid electrolyte not containing Mn^{2+} and conditioned by applying a constant potential of 1.3 V for 1 min before applying a cathodic scan. The charge under the first reduction peak was integrated and normalized to that with zero soak time. The normalized charge against soak time is shown in Fig. 5. The effect of scan rate on the anodic wave is shown in Fig. 6.

4. Discussion

4.1. *Initial step of Mn^{2+} oxidation*

The theoretical collection efficiency observed at the rising portion of the ring current (Fig. 1) suggested that initial oxidation of Mn^{2+} did not result in MnO_2 deposition. The possibility of forming solid MnO_2 in the electrolyte was also ruled out because reduction of MnO_2 at the ring potential was a one-electron process which would yield one-half of the theoretical collection efficiency. A precursor of MnO_2 such as a Mn^{3+} ion could be the initial oxidation product. The adsorption of Mn^{2+} onto platinum surfaces did not appear to occur. Voltammograms from -0.15 to 1.10 V were obtained of the platinum disc electrode at 80° C in 0.5 M sulphuric acid with and without 1 mM $MnSO_4$. There was no discernible differences between the two voltammograms which would indicate the adsorption of Mn^{2+} onto the platinum surface. The surface low oxides and high oxides which are reactive in some systems [17] were apparently not involved in Mn^{2+} oxidation. Observed similar behaviour [18] of Mn^{2+} oxidation at glassy carbon and smooth titanium electrodes, which did not have active surface oxides, supports the argument.

The first step of Mn^{2+} oxidation at a clean platinum electrode can be either a one-electron oxidation to Mn^{3+} or two-electron oxidation to Mn^{4+}. Vetter *et al.* [21] reported equilibrium potentials for the Mn^{2+}/Mn^{3+} and Mn^{3+}/Mn^{4+} systems in 15 N H_2SO_4 at room temperature to be 1.29 and 1.46 V, respectively. We studied the reaction at 80° C and above in the potential range up to 1.4 V. Oxidation of Mn^{2+} to Mn^{3+} and Mn^{4+} is certainly possible because of less activation overvoltage at a higher temperature.

Either Mn^{3+} or Mn^{4+} must stay in the solution as free ions and be detected at the ring electrode. Adsorption of these high valent manganese ions onto clean platinum is not impossible. If adsorption occurs, saturation or equilibrium must be quickly established. Mn^{4+} is not stable in the solution. It has been known that Mn^{4+} reacts with water to form $Mn(OH)_4$ which dehydrates easily to yield MnO_2 [20]. Figure 2 reveals that the initial oxidation product stayed in the solution for a long period of time without forming a MnO_2 deposit. Therefore, Mn^{4+} is less likely to be the initial oxidation product. The Mn^{3+} ions, whose stability under the experimental conditions studied has been reported in the literature [21, 22], can undergo disproportionation to yield Mn^{2+} and MnO_2. The concentration of Mn^{3+} in the electrolyte is controlled by the equilibrium

$$2Mn^{3+} + 2H_2O = Mn^{2+} + MnO_2 + 4H^+ \quad (1)$$

Solid MnOOH intermediate can be formed on electrode surfaces from hydration of Mn^{3+}

$$Mn^{3+} + 2H_2O = MnOOH + 3H^+ \quad (2)$$

The subsequent oxidation of MnOOH forms MnO_2. Reactions 1 and 2 are believed to be responsible for nucleation of MnO_2 at clean platinum surfaces. At a high anodic potential or after the induction period. Mn^{3+} is accumulated and the equilibrium is forced to the right to form MnO_2. We previously attempted to use a thin layer electrochemical cell coupled with a spectrometer to identify the intermediate [18]. However, the signal-to-noise ratio of the observed absorption band by Mn^{3+} was too poor to draw a clear conclusion.

4.2. *Growth of EMD*

Figure 1b shows a static ring current during the growth of MnO_2, suggesting a substantial constant concentration of oxidative product either as the intermediate or as MnO_2 in the electrolyte. Welsh [22] reported an equilibrium constant for Reaction 1 to be 1.6×10^7 at 90° C. The equivalent Mn^{3+} concentration under the experimental conditions in Fig. 1, calculated using this constant, was about 30 μM, or 0.3% of the bulk Mn^{2+} concentration. An observed collection efficiency on the order of 10^{-3}, or 0.6% of the theoretical value, at the ring electrode for Mn^{2+} oxidation on a growing MnO_2 surface was consistent with the calculated fraction of the equilibrated Mn^{3+} in the electrolyte. Apparently, the equilibrium involving Mn^{2+}, Mn^{3+}, and MnO_2 is sustained during the growth of EMD.

Mn^{2+} oxidation beyond the critical potential or after an induction time is a fast process and results directly in the formation of solid MnO_2. Diffusion of Mn^{2+} is a factor controlling the growth of MnO_2. The measured diffusional activation energy for Mn^{2+} in 0.5 M H_2SO_4, 44.8 kJ mol^{-1}, is in agreement with that reported by Sato *et al.* [7]. Guidelli and Piccardi [20] determined the diffusion coefficient of Mn^{2+} in 15 N H_2SO_4 to be 0.98×10^{-6} cm^2 s^{-1} at 25° C, similar to our calculated value of 1.42×10^{-6} cm^2 s^{-1}. Our value is larger because we used a more dilute sulphuric acid than did Guidelli and Piccardi.

The diffusional limiting disc current under the conditions described in Fig. 1 is calculated using the Levich equation. The results are inlaid in Fig. 1a. The

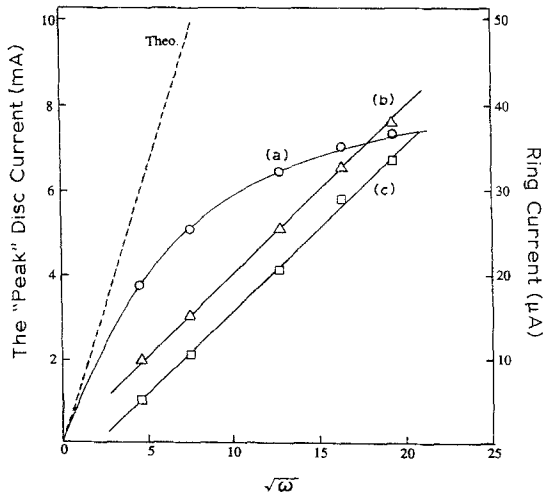

Fig. 4. Levich plots of the disc current (a) and the maximum ring currents at (b) and beyond (c) the critical potential. Data are from Fig. 1. The dashed line represents the theoretical slope.

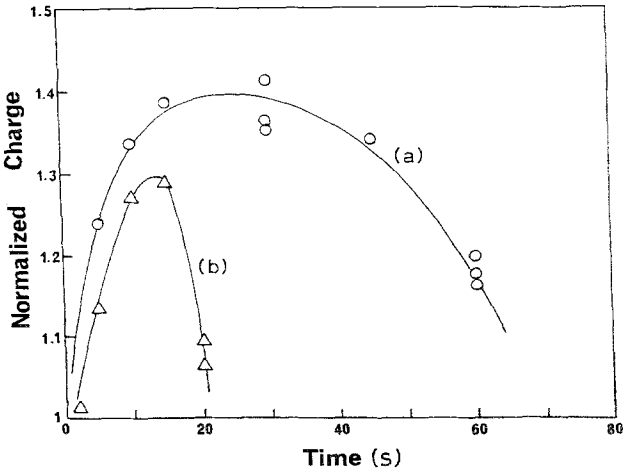

Fig. 5. Effect of open-circuit time on the reduction of MnO_2 deposit. The MnO_2 deposit is soaked in electrolyte containing (a) 10 mM, (b) 100 mM Mn^{2+} at 90°C before transferring to sulphuric acid at the same temperature for conditioning and cathodic reduction.

total charges passed in the anodic scan in Fig. 1 would generate MnO_2 deposits up to 0.4 μm thick, assuming 100% current efficiency. This thickness represented only 0.06% to 3.4% of the diffusion layer thickness, depending on rotation rate. Flow perturbation caused by the deposit was therefore neglected. At low rotation rates, the experimental results are consistent with the calculations. At high rotation rates, however, the difference between the experimental results and calculations increases with rotation rates. The same behaviour is again illustrated in Fig. 4, Levich plots for the maximum disc current, the first "peak" ring current and the maximum ring current beyond the first "peak". The maximum disc current forms a curve while the ring currents show a linear relationship with respect to the square root of rotation rates.

From Figs 1 and 4, it is evident that the r.d.s. of EMD growth changes from diffusion of Mn^{2+} to a kinetic controlled reaction. The first "peak" ring current in Fig. 1 reflects the maximum concentration of the intermediates in the electrolyte near the clean electrode surface. A linear relationship with respect to the square root of rotation rates is expected. The changes in the ring current profile during the potential scan reflects the shift in equilibrium.

MnO_2 surfaces can be chemically reduced by Mn^{2+} to form MnOOH and/or Mn^{3+} depending on the local pH and potential. Thus,

$$Mn^{2+} + MnO_2 + H^+ \longrightarrow MnOOH + Mn^{3+} \quad (3)$$

$$Mn^{2+} + MnO_2 + 2H_2O \longrightarrow 2MnOOH + 2H^+ \quad (4)$$

The concentration of Mn^{3+} should also satisfy the equilibrium in Reaction 1. MnOOH can be oxidized to MnO_2 by releasing a hydrogen ion. That is,

$$MnOOH \longrightarrow MnO_2 + H^+ + e^- \quad (5)$$

Reactions 3 to 5 are supported by the experimental observation shown in Fig. 5. Lee *et al.* [24] studied the reduction of MnO_2 in acid and concluded that the first peak in the cathodic scan was reduction of MnO_2 to MnOOH. Gosztola and Weaver [12] also gave the same conclusion in their studies. The ratio of the reduction charge to the anodic charge (Fig. 1) mentioned earlier agrees with this conclusion. Thus, integration of the charge under the first reduction peak would reflect the available amount of MnO_2 deposit for the experiment shown in Fig. 5.

In Fig. 5, the reductive charge for the deposit with zero soak time is 51.2% of the anodic charge passed. Additional reductive charge, up to 40% of that with zero soak time, is available when the MnO_2 deposit is left open-circuited in the electrolyte containing 10 mM Mn^{2+} for a short period of time. Competitive Reactions 3 and 4 occur during soak. A 40% pick up translates into a conversion of 0.06 μm thick MnO_2 to MnOOH during the establishment of the new equilibrium. Manganese apparently is picked up via Reaction 4. The subsequent conditioning at 1.3 V converts MnOOH to MnO_2, following Reaction 5, and thereby gives more charge during the cathodic reduction. For a prolonged soak, the MnO_2 surface is converted to MnOOH to slow down Reaction 4. Mn^{3+} diffuses away to force dissolution of MnOOH to re-establish equilibrium (Reaction 2). This would result in loss of charge. With a high Mn^{2+} concentration (curve b, Fig. 5), the MnO_2 surface is quickly converted to MnOOH. Consequently, pick-up of manganese via Reaction 4 is less. Loss of capacity occurs earlier because more Mn^{3+} is needed to satisfy the equilibrium.

4.3. *Considerations in support of the proposed mechanism*

Overall, Mn^{2+} oxidation is a two-electron process. The different current decays of Mn^{2+} oxidation at various rotation rates in the RRDE experiment (Fig. 1) can be explained by Reactions 3 to 5, a *ce* mechanism. At low rotation rates, Mn^{2+} ions at the surface of MnO_2 diminish due to slow diffusion from the bulk electrolyte. Reaction 5 becomes a fast step, compared to Reactions 3 and 4. Therefore, diffusion of Mn^{2+} to the electrode surface controls the reaction

and the theoretical constant limiting current is established (Figs 1 and 4). The electrode surface is dominated by MnO_2 and a static Mn^{3+} concentration is achieved according to the equilibrium expressed in Reaction 1. At high rotation rates, the MnO_2 surface is dominated by MnOOH, due to the competition of Reactions 3 and 4. The r.d.s. gradually shifts to Reaction 5, the *e* step. Solid MnO_2 formed in Reaction 5 is quickly converted to MnOOH and a layer of MnOOH builds up. Hydrogen ions from Reaction 5 have to diffuse through the solid layer of the deposit as the oxidation proceeds. In-solid diffusion of H^+ and perhaps charge transfer through the less conductive MnOOH would result in the decay of disc current. Thermodynamically, MnOOH may not be a favourable product at the anodic potential. However, kinetic hindrance including a large *iR* drop through the EMD deposit and slow in-solid diffusion of H^+ may change the local potential and result in the formation of MnOOH.

The rise of ring current after the first peak, which basically reflects the increasing Mn^{3+} concentration, must be the result of the new equilibrium involving solid MnO_2 and MnOOH intermediate, such as shown in Reactions 2 and 3. This rise would then be balanced at high overpotentials when Reaction 5 is accelerated. This would cause the reduction of the intermediate concentration and the decay of the ring current to form the "second peak". Another possible cause of the "second peak" is that when a thick layer of MnOOH is building up, diffusion of H^+ in the solid layer becomes the r.d.s. which results in decay of both disc and ring currents. Mn^{2+} ions are too big to diffuse in solid MnOOH [25, 26]. The transition of r.d.s. seems to occur at a rotation rate of about 400 r.p.m. under the conditions described in Fig. 1. Assuming that the diffusion rate of Mn^{2+} matches the conversion rate of MnOOH to MnO_2 at this rotation rate and the surface concentration of MnOOH is 1.6×10^{-9} mol cm^{-2}, the first order rate constant of Reaction 5 is calculated to be $40\,s^{-1}$.

Figure 6 shows a premature decay of the oxidation current at low scan rates and a shift of current profile to more positive potentials at high scan rates. Theoretically, the same diffusion limited current should be reached irrespective of scan rate in the RDE experiment. The shift of the disc current profile to a more positive potential at high scan rates agrees with the hypothesis of a slow kinetic process in the early stages of Mn^{2+} oxidation. The slope of the rising current portion is about the same regardless of the scan rate, indicating fast charge transfer at the growing MnO_2 surface. The changes in the shape of the current profile with respect to the scan rate agrees with the above mechanism. At high scan rates, less charge is passed and the MnO_2 layer is thinner. The in-solid diffusion is less significant and the reaction is controlled by Mn^{2+} diffusing in the bulk electrolyte. The disc current profile is therefore flatter. At low scan rates, more charge is passed to form a thicker MnO_2 layer as well as the intermediate layer. When the in-solid diffusion is taking control, the disc current starts deviating from

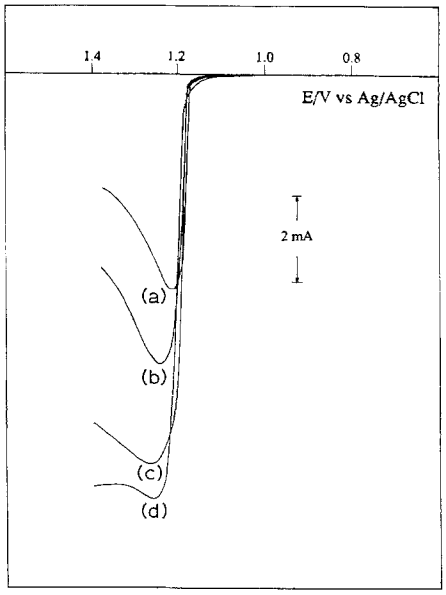

Fig. 6. CV's for Mn^{2+} oxidation at the platinum disc electrode in 0.5 M H_2SO_4 with 10 mM $MnSO_4$ at 90° C. The scan rates are (a) 5, (b) 10, (c) 20, and (d) $30\,mV\,s^{-1}$. The rotation rate is 2500 r.p.m.

the diffusion current of Mn^{2+} from the bulk electrolyte and results in a peak shape. The thickness of the MnO_2 deposit at the "peak" in Fig. 6 was calculated from the anodic charge to be 0.079, 0.083, 0.066, and 0.050 μm for scan rates from low to high, respectively. Such thickness is small compared to the thickness of the diffusion layer of about 15 μm. Flow perturbation can thus be ignored. It is interesting to note that anodic current decays when the deposit thickness becomes greater than about 0.05 μm. This value is consistent with that derived from Fig. 5 for the thickness of MnO_2 converting to MnOOH during soak.

Based on the proposed mechanism, the maximum current to practice EMD deposition is related to the diffusion rate of H^+ in the solid. It is the general consensus that a current density of about $10\,mA\,cm^{-2}$ is the highest limit to achieve EMD deposition at 90° C with 100% current efficiency. The diffusion coefficient of H^+ in solid MnO_2 has been determined to be $2.0 \times 10^{-12}\,cm^2\,s^{-1}$ at 90° C [25]. Assuming that the diffusion coefficient of hydrogen ions in the solid MnOOH phase is the same as that in MnO_2, the diffusion thickness required to achieve $10\,mA\,cm^{-2}$ can be calculated if the regional H^+ concentration is known. The maximum regional H^+ concentration, derived from the MnOOH lattice data [27], is about $0.045\,mol\,cm^{-3}$. The maximum thickness of the MnOOH layer is calculated using Fick's first law to be 0.02 μm. This value is the same order of magnitude as that derived from Figs 5 and 6.

An increase in the temperature of the solution from 80 to 95° C resulted in an increase in the oxidation current at the disc but did not substantially change the shape of the current profile. The two ring "peaks" both decreased as the temperature increased. This observation is also in agreement with the above *ce* mechanism. At a higher temperature, equilibrium

(Reaction 1) shifts to the right and the Mn^{3+} concentration is reduced. Also, Reaction 5 is accelerated. The shape of the disc current profile is still controlled by the equilibrium between Mn^{2+}, Mn^{3+} and MnO_2, and the building of a MnOOH layer.

5. Conclusions

Oxidation of Mn^{2+} to Mn^{3+} followed by disproportionation of Mn^{3+} to form MnO_2 nuclei initiates EMD deposition. More evidence, however, is needed to confirm the identity of the intermediate. On the growing MnO_2 surface, Mn^{2+} oxidation to MnO_2 follows a *ce* mechanism in which the MnO_2 surface is reduced by Mn^{2+} to form a MnOOH intermediate. The subsequent electrochemical oxidation of MnOOH to MnO_2 results in the release of hydrogen ions. A MnOOH intermediate layer up to 0.06 μm can build up. Diffusion of hydrogen ions through the solid phase can thus become a limiting factor in this process.

Acknowledgement

The authors are grateful for the support of the RAYOVAC Corporation.

References

[1] A. Kozawa, in 'Batteries', vol. 1, (edited by K. V. Kordesch), Marcel Dekker, New York (1974).
[2] H. K. Chakrabarti and T. Banerjee, *J. Sci. Industr. Res.* **12B** (1953) 211.
[3] E. Schrier and R. W. Hoffmann, *Chem. Eng.* **61** (1954) 152.
[4] S. A. Zaretskii and E. I. Antonovskaya, *Elektrokhimiya Margantsa, Akad, Nauk Gruz. SSR* **3** (1957) 232.
[5] M. Fleischmann, H. R. Thirsk and I. M. Tordesillas, *Trans. Faraday Soc.* **58** (1962) 1865.
[6] M. Sugimori and T. Sekine, *Denki Kagaku Oyobi Kogyo Butsuri Kagaku* **37** (1969) 380.
[7] M. Sato, K. Matsuki and M. Sugawara, *Kogyo Kagaku Zasshi* **72** (1969) 1073; **73** (1970) 905.
[8] F. R. A. Jorgensen, *J. Electrochem. Soc.* **117** (1970) 275.
[9] A. Cartwright and R. L. Paul, 'Manganese Dioxide Symposium', Vol. 2, Tokyo (1980) p. 290.
[10] R. L. Paul and A. Cartwright, *J. Electroanal. Chem.* **201** (1986) 113; **201** (1986) 123.
[11] A. Grzegorzewski and K. E. Heusler, *ibid.* **228** (1987) 455.
[12] D. Gosztola and M. J. Weaver, *J. Electroanal. Chem.* **271** (1989) 141.
[13] (a) J. A. Lee, C. E. Newnham, F. S. Stone and F. L. Tye, *J. Colloid Interface Sci.* **42** (1973) 289; (b) J. A. Lee, C. E. Newnham and F. L. Tye, *ibid.* **42** (1973) 372.
[14] R. G. Burns, BMRA Symposium, Vol. 341, Brussels, Belgium, 1983 (1984).
[15] W.-H. Kao, C. W. Gross and R. J. Ekern, *J. Electrochem. Soc.* **134** (1987) 1321.
[16] W. M. Latimer, 'Oxidation Potentials', Prentice-Hall, New York (1952).
[17] W.-H. Kao and T. Kuwana, *J. Electroanal. Chem.* **169** (1984) 167; **193** (1985) 145.
[18] W.-H. Kao and V. J. Weibel, unpublished data.
[19] A. J. Bard and L. R. Faulkner, 'Electrochemical Methods', Wiley, New York (1980).
[20] R. Guidelli and G. Piccardi, *Electrochim. Acta* **13** (1968) 99.
[21] (a) K. J. Vetter and G. Manecke, *Z. Phys. Chem.* **195** (1950) 270; (b) K. J. Vetter, 'Electrochemical Kinetics, Theoretical and Experimental Aspects', Academic, NY (1967) pp. 460 and 461.
[22] J. Y. Welsh, *Electrochem. Tech.* **5** (1967) 504.
[23] P. Ruetschi and R. Giovanoli, *J. Appl. Electrochem.* **12** (1982) 109.
[24] J. A. Lee, W. C. Maskell, and F. L. Tye, *J. Electroanal. Chem.* **79** (1977) 79.
[25] W.-H. Kao, *J. Electrochem. Soc.* **135** (1988) 1317; **136** (1989) 13.
[26] P. Ruetschi, *ibid.* **131** (1984) 2737.
[27] R. G. Burns and V. M. Burns, in 'Marine Manganese Deposits' (edited by G. P. Glasby), Elsevier, Amsterdam, The Netherlands (1977).